The Astrophysical Journal, 268:370-380, 1983 May 1

AN ATTEMPT TO RESOLVE PULSAR MAGNETOSPHERES USING INTERSTELLAR SCINTILLATIONS

J. M. Cordes
Cornell University, NAIC

J. M. Weisberg
Princeton University

and

V. Boriakoff
National Astronomy and Ionosphere Center
Received 1982 May 3; accepted 1982 October 20

ABSTRACT

Interstellar scintillations of separate pulse components were measured as a test for whether the corresponding emission regions are spatially separated when radiating toward an observer. Pulse components scintillate identically within the errors, implying that the emission regions have transverse separations $\lesssim 10^3$ km. In polar cap models, such separations correspond to a limit on emission altitude of 6% of the light-cylinder radius for PSR 0525+21. In light cylinder models, the limits require that nonazimuthal velocities of the emission regions must be identical to within $\Delta v/v \lesssim 0.06$ and must be within 3° of the radial direction.

Subject headings: hydromagnetics — interstellar: matter — pulsars

I. INTRODUCTION

The resolving power of interstellar scintillations (ISS) with regard to angular size is extraordinary: at meter wavelengths, attenuation of the scintillations occurs for sources larger than about $\phi_c \sim 10^{-7}$ arcsec. Such angular resolution corresponds to an interferometer with a baseline of 20 AU. Although pulsars are sufficiently small to scintillate, they are potentially resolvable with ISS, as first pointed out by Lovelace (1970, pp. 390–391) and later by Lyne (1974) and Backer (1975). A simple way to see that pulse components may scintillate differently is to compare the critical size ϕ_c with the angular size of a pulsar's velocity-of-light cylinder, whose radius is an upper bound on the spatial separation of emission regions. These quantities are

$$\phi_{\rm LC} = r_{\rm LC}/z = 0.33 P z_{\rm kpc}^{-1} \quad \text{micro-arcsec} \qquad (1)$$

and

$$\phi_c \approx 0.2(C_N^2/10^{-4} m^{-6.67})^{-0.6} \times (f/430\ \text{MHz})^{-1.2} z_{\rm kpc}^{-1.6} \quad \text{micro-arcsec}\,, \qquad (2)$$

where P is pulsar period in seconds, $z_{\rm kpc}$ is the pulsar distance in kiloparsecs, f is the observation frequency, and C_N^2 is the level of turbulence along the line of sight. Recent studies have shown that electron density fluctuations $\delta n_e/n_e \sim 10^{-3}$ on length scales of $\sim 10^{11}$ cm are those responsible for pulsar ISS and that the fluctuations are consistent with an overall wavenumber spectrum of the form $C_N^2(\text{wavenumber})^{-\alpha}$ possibly extending over many decades in wavenumber, where $\alpha = 3.7 \pm 0.6$ (Rickett 1977; Armstrong and Rickett 1980; Armstrong, Cordes, and Rickett 1981). If $\phi_c < \phi_{\rm LC}$, then emission regions separated by a light-cylinder radius will produce diffraction patterns at the Earth, and hence scintillations, that are independent. The scaling laws of ϕ_c and $\phi_{\rm LC}$ with distance and pulsar period are such that pulsars with large periods and *large* distances are more likely to be resolved by ISS.

Whereas the notion of angular resolution is useful in comparing various astronomical techniques, a careful treatment of the resolving power of scintillations requires that we consider the spatial scale of the underlying diffraction pattern. A point source produces a scintillation diffraction pattern at the Earth whose spatial scale (transverse to the line of sight) is

$$S_I = 2.8 \times 10^4 f_{\rm GHz}^{6/5} z_{\rm kpc}^{-3/5} \times (C_N^2/10^{-4} m^{-20/3})^{-3/5} \quad \text{km}\,. \qquad (3)$$

Its meaning is as follows: A point source will produce ISS that is $100e^{-1}$% decorrelated for two observers separated by transverse distance s_I. Reciprocity dictates that two transmitters with transverse separation s_I will produce two diffraction patterns at distance z that are decorrelated by $100e^{-1}$%. Therefore two pulsar emission regions whose transverse separation is s_I *at their retarded emission times* will produce ISS at a single observatory that are decorrelated by the same amount.

It is well known that pulsar emission is associated with beams of radiation attached to rotating neutron stars. Relativistic beaming is almost certainly relevant, either because of motion along approximately radial lines (polar cap models) or because of motion in the rotational azimuthal direction at or near the light cylinder (light-cylinder models). Average pulse shapes often have several components, whose separations in time evidently correspond to angular separations in the pulsar magnetosphere. Depending on the geometry, these angular separations may further imply spatial separations which are large enough to be resolved with ISS.

In this paper we discuss scintillation observations of two pulsars that have well-defined pulse components. Scintillations are manifest as intensity fluctuations in both time and frequency, so we measured radio-frequency spectra at 10 s intervals for each pulse component. The ISS-induced corrugation of what would otherwise be a flat or nearly flat spectrum (according to pulsar phenomenology) varies on time scales that are typically minutes. If pulse components were produced at significantly spaced emission regions, then the spectra for the components would be different.

Section II outlines the details of our observations and the correlation analysis of the spectra. Section III discusses the implications of our failure to detect any difference between the ISS of the two components.

II. OBSERVATIONS AND ANALYSIS

a) *Radio Spectra of Pulsar Signals*

Measurements were made at 430 MHz using the 305 m Arecibo telescope in 1980 November. Figure 1 shows the average wave forms of the observed pulsars and the time windows in which spectra were obtained. A one-bit autocorrelator was gated so as to accumulate lagged products separately for the windows of Figure 1 over an elapsed time of ~ 10 s (four pulse periods for PSR 0525+21 and eight periods for PSR 1133+16). The resultant 252-channel power spectra extend over total bandwidths of 0.312 MHz for PSR 0525+21 and 10 MHz for PSR 1133+16. Lagged products accumulated in an off-pulse window were used to form a reference spectrum so that the instrumental spectral response could be removed. In contrast to the beam switching or frequency switching used in the spectroscopy of time-stationary sources, the temporal-switching technique provides extremely smooth baselines in the spectra that are free from standing wave effects or uncertainties due to spatially varying background emission, etc. The technique is described in some detail by Weisberg, Rankin, and Boriakoff (1979).

Denoting $A_1(f)$, $A_2(f)$, $A_{\rm off}(f)$ as the power spectra (i.e., the Fourier transforms of the sines of the autocorrelation functions of the one-bit signals) and P_1, P_2, $P_{\rm off}$ as the total power measured in the three windows, quotient spectra were computed in the standard way as

$$s_{1,2}(f) = \left[\frac{P_{1,2}\,A_{1,2}(f) - P_{\rm off}\,A_{\rm off}(f)}{A_{\rm off}(f)(P_{1,2} - P_{\rm off})}\right], \tag{4}$$

where 1 and 2 correspond to the two pulse-windows. Figure 2 shows sequences of spectra for the two pulsars.

We must address the question of whether the one-bit autocorrelation technique, which is predicated on Gaussian signals with stationary statistics, can be used on pulsar signals with impunity. Pulsar intensities vary on time scales as short as microseconds with decidedly non-Gaussian statistics. However, it has been demonstrated (Cordes 1976*a*; Hankins and Boriakoff 1979; Cordes and Hankins 1979) that pulsar signals are accurately described as slow modulations (of arbitrary statistics) of Gaussian noise. If the modulation is approximately constant over a time equal to the maximum lag in the ACF, then the assumption of Gaussian statistics becomes a good one. One must still contend with the intensity fluctuations within the 10 s integration period. As shown in the Appendix, the net effect of these is to cause the mean levels of the quotient spectra to be in error. In our analysis of the derived spectra, we subtract mean levels, so fluctuations are of no consequence.

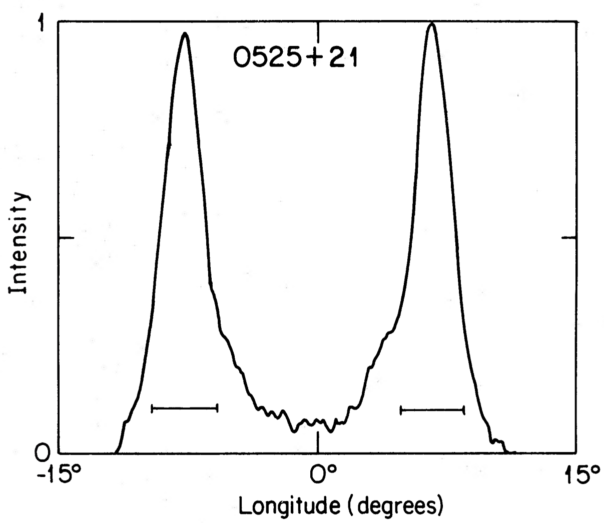

FIG. 1*a*

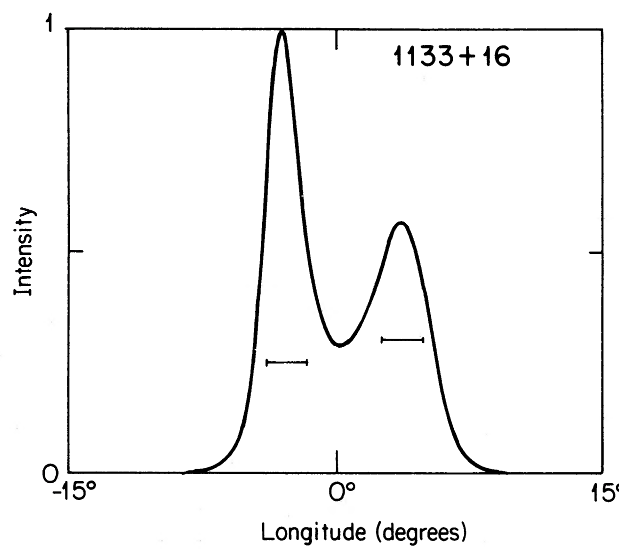

FIG. 1*b*

FIG. 1.—Wave forms of PSR 0525+21 and PSR 1133+16. Horizontal bars designate the windows in which spectra were separately obtained.

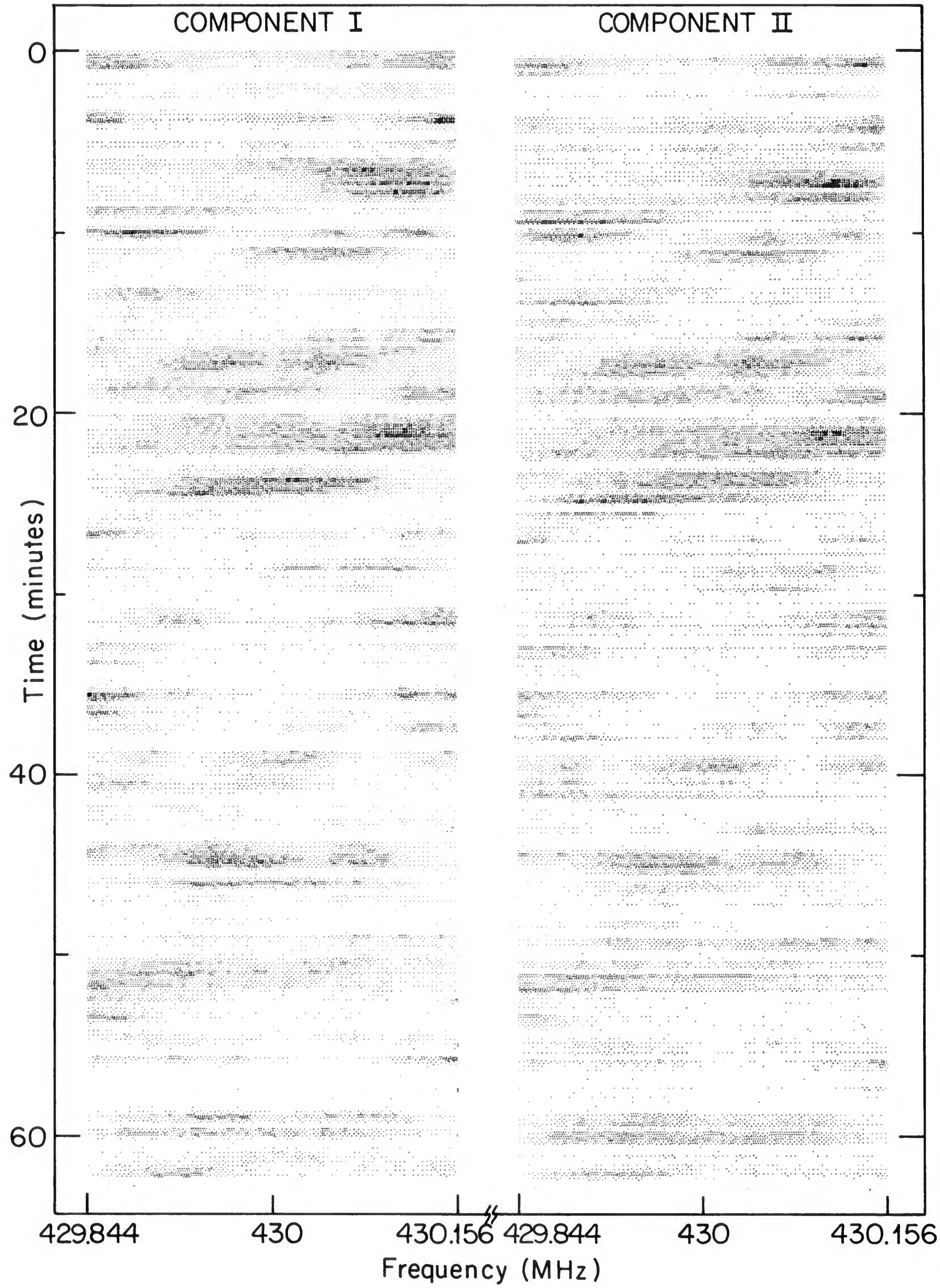

FIG. 2a

FIG. 2.—Spectra versus time for PSR 0525+21 (Fig. 2a) and PSR 1133+16 (Fig. 2b). The left- and right-hand sides are the respective spectra for the sampling windows designated in Fig. 1. For PSR 0525+21, blank spots of approximately 10 s duration are caused by episodes of pulse nulling. For the purposes of the display here, the spectra are normalized to unit area and scaled by T_{psr} $(T_{psr}^2 + T_{sys}^2)^{-1/2}$, where T_{sys} and T_{psr} are respectively the system and pulsar temperatures. Such scaling removes the effects of broad-band intensity fluctuations intrinsic to the pulsar and keeps low signal-to-noise spectra ($T_{psr} \ll T_{sys}$) from dominating the display. There are eight gray-scale levels, with white corresponding to samples that are less than 12.5% of the maximum for the entire plot.

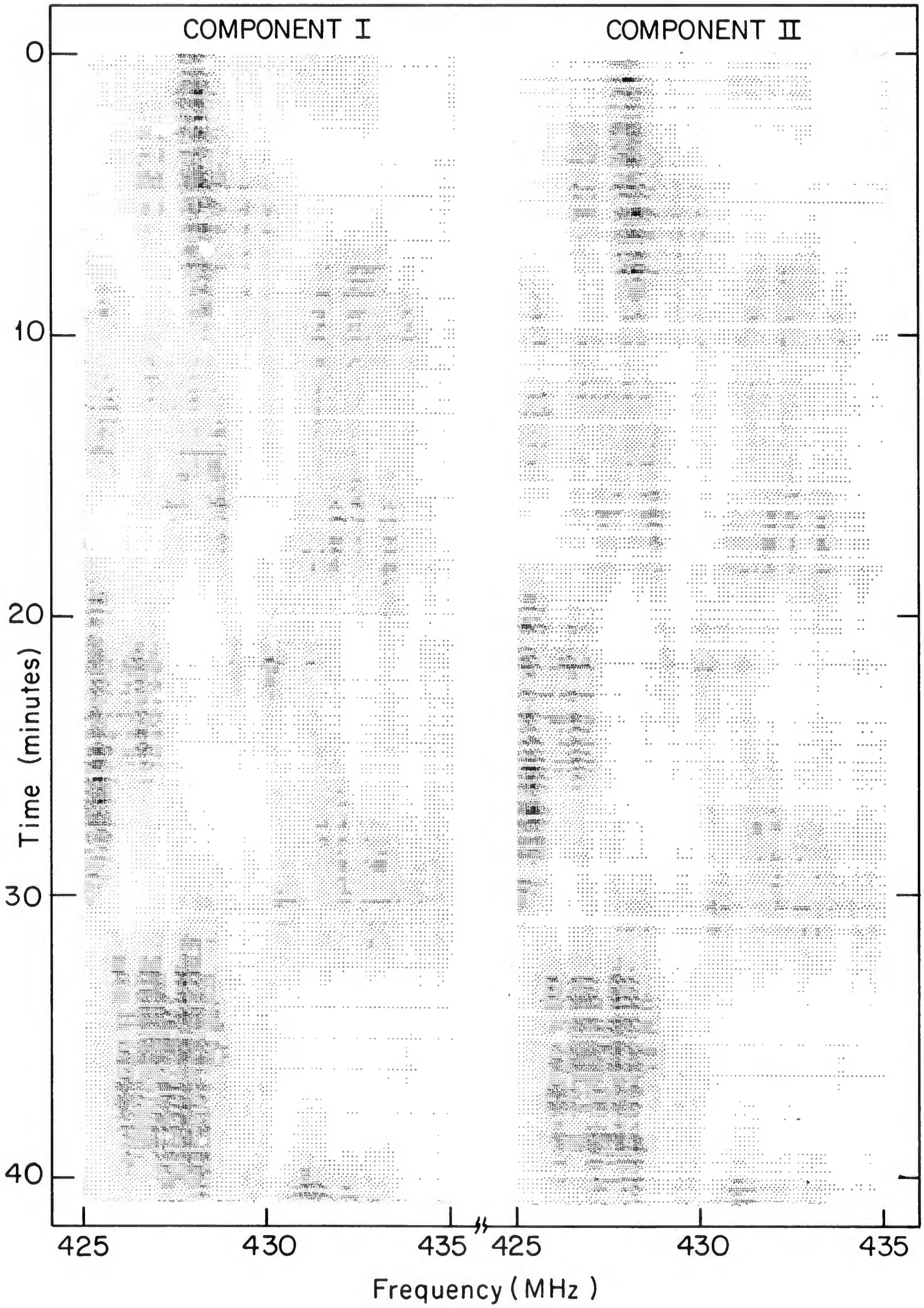
COMPONENT I
COMPONENT II
0
10
20
30
40
Time (minutes)
425
430
435
425
430
435
Frequency (MHz)

FIG. 2b

b) Correlation Functions of Pulsar Spectra

Instantaneous spectra show scintillation-induced frequency structure that varies on time scales considerably longer than an integration time of ~10 s. From the spectra we are interested in two quantities: (1) the characteristic bandwidth of the frequency structure and (2) the correlation coefficient of the spectra for the two pulse components. Both quantities were obtained from auto- and cross-correlation functions of the spectra, defined according to

$$C_{jk}(\delta f) = \left\{ \sum_l w_l \sum_f [s_{jl}(f + \delta f) - \bar{s}_{jl}] \times [s_{kl}(f) - \bar{s}_{kl}] \right\} \Big/ \sum_l w_l , \quad (5)$$

where j and k label the window, the summation over l is over a set of spectra,

$$\bar{s}_{jl} \equiv \frac{1}{N} \sum_f s_{jl}(f)$$

is the mean spectral power level, and δf the frequency lag. The weights were $w_l = T_p^2$, where T_p is the pulsar temperature of the lth spectrum. The autocorrelation functions of the spectra for the two windows are therefore

$$\mathrm{ACF}_1(\delta f) \equiv C_{11}(\delta f) ,$$
$$\mathrm{ACF}_2(\delta f) \equiv C_{22}(\delta f) ,$$

and the cross-correlation function is

$$\mathrm{CCF}(\delta f) \equiv C_{12}(\delta f) .$$

Figures 3 and 4 show the correlation functions for the two pulsars we observed. For a sufficiently long integration and apart from different normalizations, the two ACFs should be identical owing to ergodicity. The spikes in the ACFs at zero lag are absent in the CCF because they are due to radiometer noise that is uncorrelated between the two windows. Aside from the spikes, the CCF may or may not have the same shape as the two ACFs, depending on whether scintillations are identical in the two windows. The width of the ACFs represents the characteristic bandwidth of the scintillations. We will take the half-width at half-maximum (HWHM) (reckoned from the ACF peak after removing the zero-lag spike) as the so-called decorrelation bandwidth, Δf_{ISS}. In the next section we will use Δf_{ISS} to infer the spatial scales of the diffraction patterns for the lines of sight that we observed. The correlation coefficient of the ISS for the two pulse components is, as a function of frequency lag,

$$\rho(\delta f) \equiv \mathrm{CCF}(\delta f)/[\mathrm{ACF}_1(\delta f)\mathrm{ACF}_2(\delta f)]^{1/2} . \quad (6)$$

If scintillations are perfectly correlated between the two windows, then, apart from noise, $\rho(\delta f)$ is identically unity, except at zero lag where the noise spikes of the ACFs cause incorrect normalization. The spikes are evident in the correlation functions for PSR 0525+21 but are absent in those for PSR 1133+16 because the signal-to-noise ratio is much larger. The intrinsically noiselike nature of the pulsar signal should also produce spikes at zero lag, (Cordes and Hankins 1979), but these are smaller than scintillation features in the correlation functions by a factor of (intrinsic modulation time)/(net integration time) $\lesssim 0.02$, where the intrinsic modulation time is that corresponding to micropulse emission which is ~1 ms for PSR 1133+16 and ~4 ms for PSR 0525+21. Some subtleties of the correlation analysis can cause the shapes of the three correlation functions to differ slightly even if ISS is perfectly correlated between the two channels. One consequence of the one-bit correlation technique is that the derived spectra will be biased from their true shapes by an amount that depends on the signal-to-noise ratio (see Appendix). Since this ratio is different in the two windows, we expect some slight differences in shape. Second, the correlation functions in equation (5) have zero area; therefore, they must

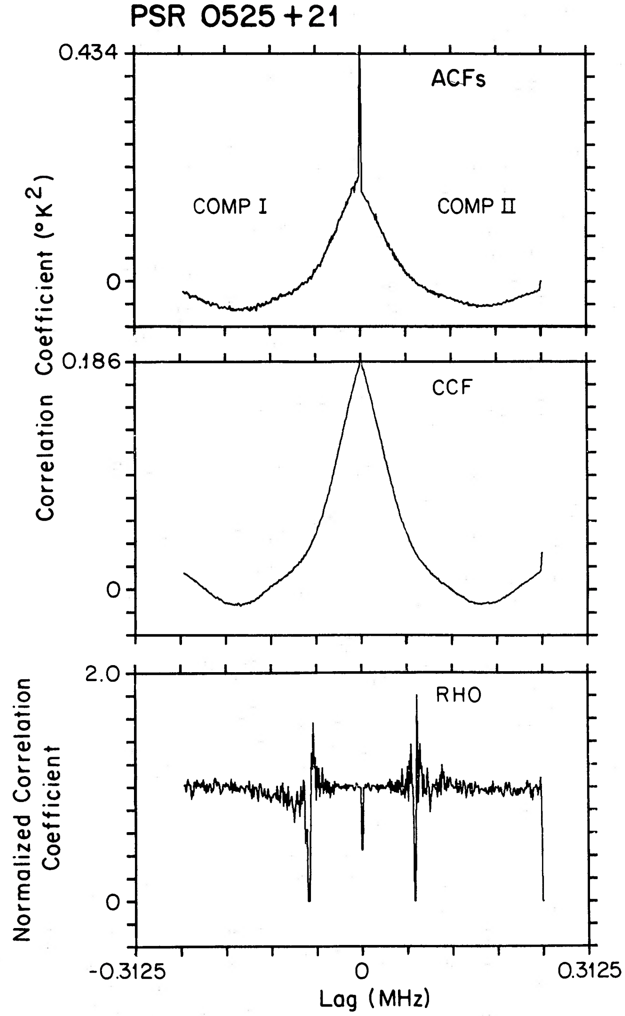

FIG. 3.—Correlation functions for PSR 0525+21. The autocorrelation function of one window is plotted for positive lags, the other for negative lags. The quotient correlation function, $\rho(\delta f)$, is unity if scintillations are perfectly correlated for the two pulse components.

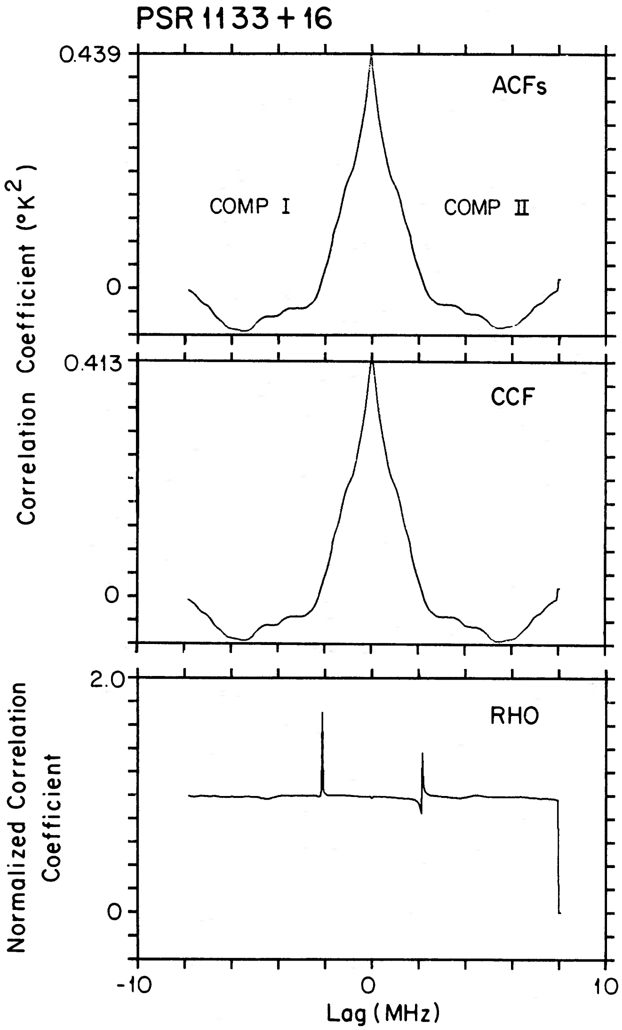

FIG. 4.—Correlation functions for PSR 1133+16

cross zero and, because of slight biasing of the spectra, the zero crossings of correlation functions will be at slightly different lags. The plots of $\rho(\delta f)$ in Figures 3 and 4 are consistent with values of unity except near the lags of zero crossing, and we presume that the deviations from unity are solely instrumental effects. By using values of $\rho(\delta f)$ away from the lags of zero crossing, we find average values of ρ as listed in Table 1 along with the decorrelation bandwidths.

III. LIMITS ON SPATIAL SEPARATIONS OF EMISSION REGIONS

In order to use our measurements to constrain pulsar geometry, we must quote some results of scintillation theory that are relevant to extended media in the strong multiple scattering limit. In this limit, the central limit theorem predicts that scintillations are 100% modulated (rms intensity equal to the mean) because the electric field is normally distributed (Rickett 1977). Lee and Jokipii (1975) derive the second moment of the scalar field,

$$\Gamma_{1,1}(\zeta, z) \equiv \frac{\langle u(\boldsymbol{r}, z)u^*(\boldsymbol{r} + \boldsymbol{\zeta}, z)\rangle}{\langle |u(\boldsymbol{r}, z)|^2\rangle}, \qquad (7)$$

where u is the scalar electric field and the asterisk denotes complex conjugate; z is the distance along the line of sight between source and observer, and $\boldsymbol{r}$ and $\boldsymbol{\zeta}$ are vectors in the plane transverse to the line of sight at distance z. For power-law electron density irregularity spectra of slope α, Lee and Jokipii obtain

$$\Gamma_{1,1}(\zeta, z) = \exp[-(\zeta/\zeta_c)^{\alpha-2}] \quad (2 < \alpha \leq 4) \qquad (8)$$

which is valid for ζ^{-1} being both much greater than the low wavenumber cutoff and much less than the high wavenumber cutoff and where ζ_c is the spatial scale of the diffraction pattern. The Fourier transform of $\Gamma_{1,1}$ is the apparent brightness distribution of a point source as viewed through the interstellar medium. Multipath propagation causes temporal smearing of a pulse over a time

$$\Delta t_{\rm ISS} = z\theta_c^2/2c, \qquad (9)$$

a relation which holds if θ_c is given by $\theta_c \zeta_c = \lambda/2\pi$ (eq. [60] of Lee and Jokipii). Although equation (9) was first derived for the case of scattering in a thin screen whose thickness is much smaller than the distance to the source, Lee and Jokipii have expressed their results for a thick extended medium such that equation (9) is still applicable and where z is the distance to the source rather than to the scattering screen. It is well known that the temporal broadening time $\Delta t_{\rm ISS}$ is related to the decorrelation bandwidth $\Delta f_{\rm ISS}$ by the uncertainty relation (Rickett 1977)

$$2\pi\Delta f_{\rm ISS}\,\Delta t_{\rm ISS} = 1. \qquad (10)$$

Finally, by invoking the strong, multiple scattering limit,

TABLE 1

SCINTILLATION MEASUREMENTS OF TWO PULSARS AT 430 MHz

Pulsar	Integration Time (min)	Spectral Resolution (MHz)	Decorrelation Bandwidth $\Delta f_{\rm ISS}$ (MHz)	Correlation Coefficient of components ρ
0525+21	30	0.0012	0.05	1.0 ± 0.003
1133+16	47	0.040	~ 1.0	1.0 ± 0.003

it is possible to express the covariance function of the intensity, $I(\mathbf{r}, z)$,

$$\Gamma_{\Delta I}(\Delta \mathbf{s}, z) \equiv \frac{\langle I(\mathbf{r}, z) I(\mathbf{r} + \Delta \mathbf{s}, z)\rangle - \langle I(\mathbf{r}, z)\rangle^2}{\langle I(\mathbf{r}, z^2)\rangle}, \quad (11)$$

in terms of $\Gamma_{1,1}$:

$$\Gamma_{\Delta I}(\Delta \mathbf{s}, z) = |\Gamma_{1,1}(\Delta \mathbf{s}, z)|^2, \quad (12)$$

where $\Delta \mathbf{s}$ is a spatial lag.

By expressing

$$\Gamma_{\Delta I}(\Delta \mathbf{s}, z) = \exp[-(\Delta s/s_I)^{\alpha-2}],$$

we find that s_I, the e^{-1} spatial scale of the diffraction pattern, is given by $s_I = \zeta_c 2^{-1/(\alpha-2)}$. Then, expressing ζ_c in terms of $\Delta f_{\rm ISS}$ by using equations (9) and (10), we have

$$s_I = (cz\Delta f_{\rm ISS}/4\pi f^2)^{1/2} 2^{-1/(\alpha-2)}. \quad (13)$$

Equation (13) holds for the case of scattering of plane waves in a medium of homogeneous turbulence. For a point source, the right-hand side should be multiplied by $(\alpha - 1)^{1/2}$ if the turbulence is homogeneous (Rickett 1977), which appears to be a good assumption for both pulsars considered here (J. M. Cordes, J. M. Weisberg, and V. Boriakoff, in preparation). We have included this correction in what follows, but we have ignored the fact that equation (9) gives a value for $\Delta t_{\rm ISS}$ that is not precisely the e^{-1} width of the temporal broadening function. The correction for this amounts to multiplying the right-hand side of equation (13) by ~ 1.15. We note that there is some dispute as to whether the fourth moment can be expressed in terms of (second moment)^2 (Lerche 1979) even in the strong multiple-scattering limit. The error in doing so amounts to at most a 10% uncertainty in the width s_I that is calculated in equation (13). Consequently it is of little importance here.

We can relate the theoretical *spatial* correlation function of equation (12) to the empirical *frequency* correlation function $\rho(\delta f)$ (cf. eq. [6]) by recognizing that the zero-lag value, $\rho(\delta f = 0)$, must be equal to $\Gamma_{\Delta I}(\Delta s, z)$. Our procedure has been to use nonzero lag values of ρ to infer that $\rho(0) \approx 1$, and from this fact we can put limits on the transverse separation of the emission regions. In principle we could also have used information contained in the temporal correlation function of the data (B. J. Rickett, private communication). That is, we could have computed the empirical correlation function of equation (5) with the lth spectrum of one pulse component multiplied by the $(l + \Delta l)$th spectrum of the other pulse component and then determining the time lag, $\tau_{\max} = 10\Delta l$ s, of maximum correlation. By further assuming that the scattering medium is "frozen" over a time $> \tau_{\max}$ and that the relative velocity of the medium with respect to the pulsar is $\mathbf{v}$, it can be shown that the emission regions must have a transverse separation $\Delta s_\perp = (\mathbf{v} \cdot \Delta \mathbf{s})\tau_{\max}/\Delta s$. For $\tau_{\max} \lesssim 10$ s and velocities ~ 100 km s^{-1} one obtains limits on $\Delta s_\perp$ that are similar in magnitude to those obtained below using the frequency correlation function. Use of the temporal lag method requires knowledge of the direction and magnitude of the velocity, which are uncertain, so therefore we have used only the frequency correlation function to limit the separations of emission regions.

The correlation coefficients in Table 1 are consistent with values of unity, but we can define a 3 σ lower limit on the correlation coefficient as $1 - \epsilon$, where $\epsilon \approx 0.01$. We have

$$\Gamma_{\Delta I}(\Delta \mathbf{s}, z) \geq 1 - \epsilon. \quad (14)$$

For $\epsilon \ll 1$ this becomes a limit on Δs, the spatial separation of the emission regions:

$$\Delta s \leq s_I \epsilon^{1/(\alpha-2)}. \quad (15)$$

Table 2 lists the upper limits on Δs for $\alpha = 11/3$.

We note that the slope, α, of the electron-density irregularity spectrum is not known with certainty. However, recent observations (Armstrong and Rickett 1980; Wolszczan, Bartel, and Sieber 1981) favor power-law spectra with slopes less than 4 and do not support a Gaussian spectrum with a single scale size for the irregularities. As far as observables are concerned, the Gaussian case is degenerate with an $\alpha = 4$ power-law spectrum.

a) Polar Cap Models

The so-called polar cap models (Manchester and Taylor 1977) have as a common element a source of charged particles at the magnetic polar cap with radiation subsequently produced *somewhere* along the particles' trajectories along the curved field lines of an approximately dipolar magnetic field.

Whereas there is no consensus as to how and where radiation is produced, there is compelling observational evidence in support of radiation being produced by a time-average hollow-cone beam centered on the dipolar axis (Komesaroff 1970; Cordes 1981). The model is shown schematically in Figure 5 where, for simplicity,

TABLE 2

LIMITS ON EMISSION REGION GEOMETRY

					Polar Cap Model		Light-Cylinder Model	
Pulsar	ϵ	z (kpc)	Δs (km)	$\Delta\theta_w$	$r_{\rm em}$ (km)	$r_{\rm em}/r_{\rm LC}$	$\Delta\beta$	$\Delta\alpha$
0525+21	0.01	2.0	850	14°	$<10^{4.04}$	<0.06	$<10^{-2.0}$	<0°.6
1133+16	0.01	0.2	1100	6°.4	$<10^{4.5}$	<0.53	$<10^{-1.3}$	<2°.9

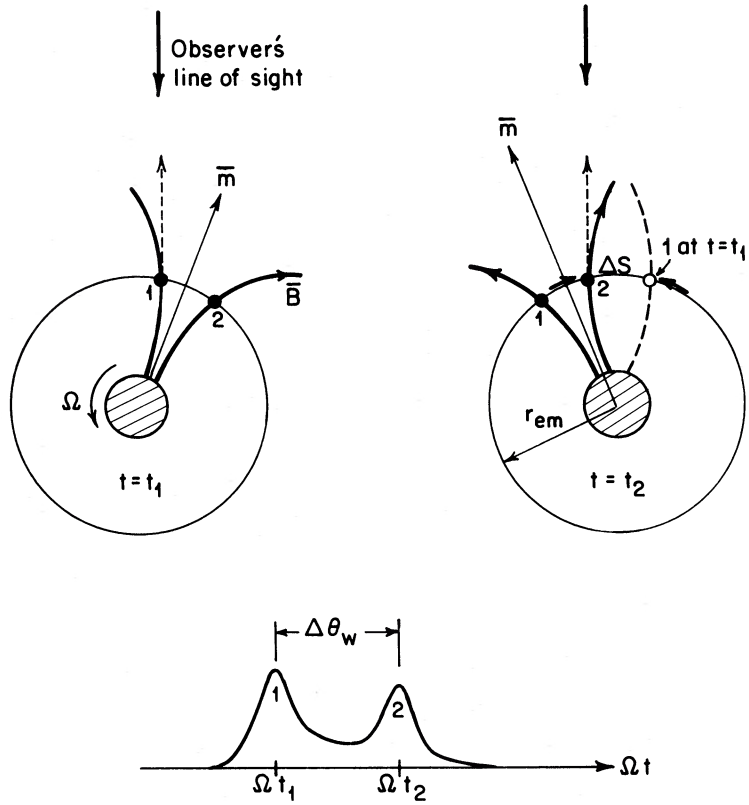

FIG. 5.—Geometry of polar cap models. A magnetic moment *m* perpendicular to the spin axis is assumed. Emission regions 1 and 2 at radius r_{em} produce pulse components 1 and 2. The emission regions radiate toward the observer from locations that have a transverse separation Δs.

the dipole moment is assumed to be perpendicular to the rotation axis. A double-lobed average pulse shape is produced if the line of sight cuts through the beam sufficiently close to the magnetic pole (see, e.g., Fig. 1 of Backer 1976). The two lobes originate from opposite sides of the magnetic pole. Under the assumption that radiation is relativistically beamed along the particles' trajectories (i.e., tangentially to the field lines), then it can be shown that the emission regions at the times they respectively beam toward Earth are separated by a distance (transverse to the line of sight)

$$\Delta s = r_{em}\,\Delta\theta_w/3\ , \tag{16}$$

where r_{em} is the emission radius and $\Delta\theta_w$ is the observed separation of pulse components expressed in radians. Equation (16) follows by assuming dipolar field geometry for which the local tangent vector at position (r, θ) makes an angle $3\theta/2$ with respect to the dipolar axis.

An upper limit on the radius of emission follows by combining equations (15) and (16):

$$r_{em} \leq (3s_I/\Delta\theta_w)\epsilon^{1/(\alpha-2)}\ . \tag{17}$$

Table 2 lists these upper limits for a turbulence spectrum with slope $\alpha = 3.7$.

The limits $r_{em}/r_{LC} < 0.06$ for PSR 0525+21 and <0.53 for PSR 1133+16 derived here can be contrasted with those derived from aberration-retardation effects (Cordes 1978). The aberration-retardation limits are based on the polar cap models with one additional assumption: that the emission frequency is mapped into radius r_{em} by virtue of a density-dependent plasma instability. Such emission causes a spread in arrival times of pulses at different frequencies over and above that caused by dispersion in the interstellar medium. Upper bounds on the aberration-retardation effect convert to limits on emission radii. These limits are $r_{em}/r_{LC} \lesssim 0.03$ for PSR 0525+21 and $r_{em}/r_{LC} \lesssim 0.01$ for PSR 1133+16. Although these limits are superior to the scintillation-derived ones and have important consequences for the physics of pulsar magnetospheres (Matese and Whitmire 1980; Ruderman 1981), they involve more assumptions than the ISS limits. The scintillations of PSR 0525+21 yield a strong limit on the growth rate of any instability that results in emission at the observation frequency. The instability must have caused significant plasma fluctuations in the travel time from the neutron star surface to the emission radius, which, for PSR 0525+21, amounts to ~ 36 ms. This conclusion holds regardless of whether emission frequency is mapped into radius.

b) Light Cylinder Models

Light cylinder models share the property that the *primary* source of particle acceleration is rotation of plasma coaxial with rotation of the neutron star. Double pulse components may be produced by emission regions at different azimuthal angles in the equatorial plane or by emission regions above and below the equatorial plane (Gold 1974). In the latter case, the ISS observations imply that emission must be within a distance $\Delta s \ll r_{\mathrm{LC}}$ of one another. If both emission regions are in the equatorial plane (e.g., Ferguson 1981), then the constraints depend on the particular geometry that is assumed. Simple circular motion of two emission regions at the same radius involves no spatial separation at the retarded emission times, so the ISS measurements are uninteresting. For models in which the emission regions have additional velocity components, limits can be made on the difference in magnitude or direction of those components. Suppose the emission regions have radial velocities with a difference in magnitude, $\Delta\beta = \Delta v/c$. The ISS limits on Δs then become

$$\Delta\beta \leq \gamma_r \beta_r \Delta s/r_{\mathrm{LC}} , \tag{18}$$

where $\beta_r = r/r_{\mathrm{LC}}$ and $\gamma_r = (1 - \beta_r^2)^{-1/2}$. Light cylinder models with typical values $2 \lesssim \gamma_r \lesssim 3$ imply $\Delta\beta \lesssim 10^{-2}$ for PSR 0525+21 and $\Delta\beta \lesssim 10^{-1.3}$ for PSR 1133+16. Alternatively, the velocities in the corotating frame may be nonradial with the same magnitude. Letting the difference in orientation from the radial direction be $\Delta\alpha$, we have

$$\Delta\alpha \leq \gamma_r \Delta s/r_{\mathrm{LC}} , \tag{19}$$

corresponding to angles $\Delta\alpha \lesssim 0.^\circ 6$ and $\Delta\alpha \lesssim 2.^\circ 9$ for 0525+21 and 1133+16, respectively.

We would like to thank J. Armstrong and B. J. Rickett for useful conversations. This research was supported by NSF grant AST 8103190 at Princeton University, by the CalTech President's Fund, and by the National Astronomy and Ionosphere Center, which operates the Arecibo Observatory under contract with the National Science Foundation.

APPENDIX

PULSAR SIGNALS AND ONE-BIT AUTOCORRELATION SPECTROMETERS

Let $\epsilon(t)$ be the narrow-band signal from a receiver after passage through an intermediate-frequency bandpass filter and after being mixed to baseband [i.e., $\epsilon(t)$ is proportional to the slowly varying part of the electric field selected by the polarization of the feed antenna and receiver bandpass; see Cordes 1976*b* for a further exposition]. The true spectrum is the Fourier transform of the autocorrelation function (ACF):

$$R_\epsilon(\tau) = \sum_t \epsilon(t)\epsilon(t + \tau) . \tag{A1}$$

If $\epsilon(t)$ is a stationary Gaussian random process, then the ACF of sgn $\epsilon(t)$,

$$R_1(\tau) = \sum_t \operatorname{sgn} \epsilon(t) \operatorname{sgn} \epsilon(t + \tau) , \tag{A2}$$

is related to R_ϵ by the Van Vleck relation (e.g., Thomas 1969)

$$\frac{\langle R_1(\tau)\rangle}{\langle R_1(0)\rangle} = \frac{2}{\pi} \sin^{-1} \left[\frac{\langle R_\epsilon(\tau)\rangle}{\langle R_\epsilon(0)\rangle}\right] , \tag{A3}$$

where the angular brackets denote ensemble average. Although pulsar signals do not immediately satisfy the assumptions that lead to equation (A3), we demonstrate here that a one-bit autocorrelation spectrometer yields a fairly accurate estimate of the true spectrum.

An empirically accurate model for pulsar signals is (after Rickett 1975 and Cordes 1976*b*)

$$\epsilon(t) = a(t)m(t) + n(t) , \tag{A4}$$

where $n(t)$ is zero-mean, band-limited Gaussian noise, $m(t)$ is zero-mean Gaussian noise whose band-limited spectrum is the desired one, and $a(t)$ is a positive semidefinite stochastic process that varies slowly with respect to both $n(t)$ and $m(t)$ and describes intensity variations which have decidedly non-Gaussian statistics. The additive noise, $n(t)$, is due to receiver and background sky noise. It is clear from equation (A4) that if $n(t) = 0$ (i.e., infinite signal-to-noise ratio), then

$$\operatorname{sgn} [\epsilon(t)] = \operatorname{sgn} [m(t)] , \tag{A5}$$

and the spectrum of the pulsar signal can be accurately retrieved through the Van Vleck correction since, by hypothesis, $m(t)$ is a stationary Gaussian process. Problems arise, however, if the signal-to-noise ratio is finite *and* time varying.

If a bandwidth Δv is analyzed then $\epsilon(t)$ is sampled at intervals $\Delta = (2\Delta v)^{-1}$ and the maximum lag is $\tau_{\max} = N\Delta$. If the pulsar intensity is nearly constant over a time $\tau_{\max}$, then the approximation

$$a(t + \tau) \approx a(t) \qquad (0 \leq \tau \leq \tau_{\max}) \tag{A6}$$

can be made. This assumption is good because here $N = 252$ and $\tau_{\max} = 0.4$ ms for PSR 0525+21 and 13 μs for PSR 1133+16. Dispersion smearing alone over the respective bandwidths of 312 kHz and 10 MHz guarantees that the characteristic time scales of $a(t)$ are respectively at least 1.7 ms and 5.1 ms. Using the approximation in equation (A6), we find that the ensemble-average one-bit ACF after summing over time is

$$\langle R_1(\tau)\rangle = \frac{2}{\pi}\sum_t \arcsin\left[\frac{I_p(t)\rho_m(\tau) + I_n(t)\rho_n(\tau)}{I_p(t) + I_n(t)}\right], \tag{A7}$$

where

$$I_p(t) \equiv \langle a^2(t)m^2(t)\rangle \tag{A8}$$

is the instantaneous pulsar intensity,

$$I_n(t) = \langle n^2(t)\rangle \tag{A9}$$

is the additive noise intensity,

$$\rho_m(\tau) \equiv \langle m(t)m(t+\tau)\rangle/\langle m^2(t)\rangle \tag{A10}$$

is the true ACF (cf. eq. [A1]) of $m(t)$, and $\rho_n(\tau)$ is the true ACF of $n(t)$. Normalization is such that $\rho_n(0) = \rho_m(0) = 1$. Note that we are also assuming that $\rho_m(\tau)$ is time independent. The physical situation we are modeling is one where the shape of the spectrum of the pulsar signal (which is determined by scattering in the interstellar medium) is constant over a 10 s integration time, so the assumption is warranted.

Recall that the angular brackets denote *ensemble* averages which, here, are not identical to time averages because $I_p(t)$ is not stationary. The sum over t describes both the integration over time within a pulse and over a set of pulses. Intensity variations are violent in the sense that $I_p(t)$ can range from zero to values large compared to the noise level even within a single pulse period. Consequently, even though the average signal-to-noise ratio

$$\frac{\sum_t I_p(t)}{\sum_t I_n(t)}$$

may be large, there will usually be times during the sum over t when it is zero. One therefore cannot take the large signal-to-noise limit of equation (A7). The additive noise is white, however, so we have (in the ideal case)

$$\rho_n(\tau) = \delta_{\tau 0}\,, \tag{A11}$$

where $\delta_{\tau 0}$ is the Kronecker delta and therefore

$$\begin{aligned}\langle R_1(\tau)\rangle &= \sum_t 1 \qquad (\tau = 0)\\ &= \frac{2}{\pi}\sum_t \arcsin\left\{\frac{\rho_m(\tau)I_p(t)}{[I_p(t) + I_n(t)]}\right\} (\tau \neq 0)\,.\end{aligned} \tag{A12}$$

It is clear that a finite signal-to-noise ratio will *bias* the derived ACF by an amount that depends on the frequency of occurrence of the signal-to-noise ratio. If this ratio is large all of the time or if it is constant, then the summation in equation (A12) can be replaced by a single term,

$$\langle R_1(\tau)\rangle \approx \frac{2}{\pi}\, T \arcsin\left[\frac{\rho_m(\tau)}{(1 + \mathrm{SN}^{-1})}\right], \tag{A13}$$

where SN is the typical ratio and T is the integration time. In this limit the resultant estimate for ρ_m,

$$\hat{\rho}_m(\tau) = \sin\left[\pi R_1(\tau)/2R_1(0)\right], \tag{A14}$$

differs from ρ_m by only a scale factor and therefore the true pulsar spectrum can be obtained. In general, however, equation (A12) shows that the spectra derived from one-bit ACFs will have shapes that depend on the signal-to-noise ratio. The most important effect is the incorrect scaling of the resultant spectrum, as modeled by Weisberg (1978). This effect is unimportant in the present analysis where we subtract the mean from each spectrum.

Biasing of spectra could be obviated if the one-bit ACF estimates and power information were recorded sufficiently often that a compensating weighting scheme could be applied. *Sufficiently often* means once every correlation time of the pulsar intensity (e.g., millisecond time scales). Such a scheme would involve obtaining $R_1(\tau)$ and $P_{\rm on} = I_p(t) + I_n(t)$ over a small integration time. Estimates of off-pulse noise power and ACF could be made over a much longer integration time if the receiver is sufficiently stable; assume, therefore, that the off-pulse statistics ρ_n and I_n are known exactly. Then estimates of ρ_m computed according to

$$\hat{\rho}_m(\tau) = \{P_{\rm on}\sin\left[\pi R_1(\tau)/2\right] - I_n\,\rho_n\}/(P_{\rm on} - I_n) \tag{A15}$$

could be accumulated without the bias discussed above. Such processing would be tedious for any realistic total integration time. Moreover, hardware presently available at the Arecibo Observatory permits only integration times that are several to many pulsar periods. Consequently a given one-bit ACF, $R_1(\tau)$, will be a linear combination of ρ_m and ρ_n with coefficients that depend on the frequency of occurrence of the signal-to-noise ratio. Since, apart from the receiver bandpass shape, the off-pulse spectrum is flat, this means that the primary effect is that the mean level of the spectrum will be unknown but the shape of the spectrum will be nearly correct.

REFERENCES

Armstrong, J. W., and Rickett, B. J. 1980, *M.N.R.A.S.*, **194**, 623.
Armstrong, J. W., Cordes, J. M., and Rickett, B. J. 1981, *Nature*, **291**, 561.
Backer, D. C. 1975, *Astr. Ap.*, **43**, 395.
———. 1976, *Ap. J.*, **263**, 202.
Cordes, J. M. 1976*a*, *Ap. J.*, **208**, 944.
———. 1976*b*, *Ap. J.*, **210**, 780.
———. 1978, *Ap. J.*, **222**, 1006.
———. 1981, in *Pulsars*, ed. W. Sieber and R. Wielebinski (Dordrecht: Reidel), p. 115.
Cordes, J. M., and Hankins, T. H. 1979, *Ap. J.*, **233**, 981.
Ferguson, D. C. 1981, in *Pulsars*, ed. W. Sieber and R. Wielebinski (Dordrecht: Reidel).
Gold, T. 1974, talk presented at the US/Australia Symposium on Pulsars, Stanford University.
Hankins, T. H., and Boriakoff, V. 1978, *Nature*, **276**, 45.
Komesaroff, M. 1970, *Nature*, **225**, 612.
Lee, L. C., and Jokipii, J. R. 1975, *Ap. J.*, **196**, 695.
Lerche, I. 1979, *M.N.R.A.S.*, **189**, 137.
Lovelace, R. V. E. 1970, Ph.D. thesis, Cornell University.
Lyne, A. G. 1974, Talk presented at the US/Australia Symposium on Pulsars, Stanford University.
Manchester, R. N., and Taylor, J. H. 1977, *Pulsars* (San Francisco: Freeman).
Matese, J. J., and Whitmire, D. P. 1980, *Ap. J.*, **235**, 587.
Rickett, B. J. 1975, *Ap. J.*, **197**, 185.
———. 1977, *Ann. Rev. Astr. Ap.*, **15**, 479.
Ruderman, M. A. 1981, in *Pulsars*, ed. W. Sieber and R. Wielebinski (Dordrecht: Reidel).
Thomas, J. B. 1969, *Statistical Communication Theory* (New York: Wiley), p. 285.
Weisberg, J. M. 1978, Ph.D. thesis, University of Iowa.
Weisberg, J. M., Rankin, J. M., and Boriakoff, V. 1979, *Astr. Ap.*, **77**, 204.
Wolszczan, A., Bartel, N., and Sieber, W. 1981, *M.N.R.A.S.*, **196**, 473.

V. Boriakoff and J. M. Cordes: National Astronomy and Ionosphere Center, Space Sciences Building, Cornell University, Ithaca, NY 14853

J. M. Weisberg: Department of Physics, Princeton University, Princeton, NJ 08544